FLOMEKO2019
18th International Flow Measurement Conference
Portugal | Lisbon | LNEC | 26-28 june 2019

The Theoretical Analysis and Waviness Profile Measurement for the Discharge Coefficient of Sonic Nozzles

Peijuan Cao[1], Chao Wang[1], Chunhui Li[2], Hongbing Ding[1]

[1]*Tianjin Key Laboratory of Process Measurement and Control, School of Electrical and Information Engineering, Tianjin University, Tianjin 300072, China*
[2]*National Institute of Metrology (NIM), Beijing100029, China*
E-mail (corresponding author): wangchao@tju.edu.cn

Abstract

To improve the measurement accuracy of sonic nozzle, the theoretical analysis and waviness profile measurement for the discharge coefficient of sonic nozzles were conducted. The theoretical discharge coefficient used a correlation model that accounts for both viscous effects due to the boundary layer along the nozzle wall ($C_{d,1}$), and the axisymmetric sonic line in the core region ($C_{d,2}$). Firstly, the inner surface coordinates of one sonic nozzle with nominal throat diameter of 7.45 mm were measured by CMM of NIM, including the throat diameter d and curvature radius R_c. The curve profile, roundness and waviness of the overall and local geometric contours are evaluated by using the data of CMM t and the perfect evaluation criteria about nozzle profile were proposed. Lastly, the R_c was used in calculating the theoretical discharge coefficients, $C_{d,th}$, while the d was used in calculating the experimental discharge coefficients, $C_{d,exp}$. The results showed the overall consistency between $C_{d,exp}$ and $C_{d,th}$ is better than 0.11% in the range of Reynolds number from 4.45×10^5 to 1.26×10^6.

1. Introduction

The sonic nozzle (SN) standard facilities were established in many countries for precise measurement and control of the gas flow, especially for natural gas, because the natural gas is more and more widely used as the clear energy. The crucial parameter of SN is discharge coefficient, which defined as a dimensionless ratio of the actual mass flow-rate to the ideal mass flow-rate. When the SN is used as the transfer standard for flow measurement, it is necessary to obtain the discharge coefficient through actual calibration or theoretical calculation.

Many of the pioneering works for SN were investigated during the 1960s and 1980s, when numerous theoretical flow models were proposed for predicting the discharge coefficient of SN. The throat diameter d and the inlet curvature radius R_c are the key geometric parameters to calculate the experimental discharge coefficient $C_{d,exp}$ and theoretical discharge coefficient $C_{d,th}$. The value of $C_{d,exp}$ is usually calibrated by the primary gas flow standard facility (e.g. pVTt or Mt facility) with the expanded uncertainty of 0.05%~0.10% (k=2). However, the primary standard facility has many inconveniences, such as long waiting time, limited flow rate range and so on. In order to avoid these shortcomings, the $C_{d,th}$ is predicted by theoretical formula to realize the direct measurement of gas flow [1]-[7].

In 2005, the latest edition of ISO 9300 standard clearly specifies the geometry of SN. As shown in Fig.1, the ideal contour of SN is composed of a standard section and a diffusion section, and the arc section is tangent with diffuser section at point B, while the diffuser angle θ is within (2.5°~6.0°). The profile transition between the standard section and the diffusion section is smooth, burr-free. In fact, it is difficult to meet the requirement of very low surface roughness for normally machined nozzles, especially for the entrance section. For the normally machined nozzles, it machined by a lathe and surface polished to achieve the desired smoothness of surface roughness less than $1.5\times10^{-5}d$, conforming to specification of ISO 9300. Unfortunately, in the process of polishing, the original ideal shape will be changed. Therefore, it is necessary to measure the geometrical profile of the SN in order to improve the prediction and experimental accuracy of the $C_{d,th}$ and $C_{d,exp}$.

In this study, the variation of the discharge coefficient of SN is analysed when the flow is in the laminar boundary layer. Firstly, the coordinate measuring machine (CMM) was used to measure the contour profile of sonic nozzles with d=7.45 mm, and corresponding the evaluation criterion was established, including curve profile, roundness and waviness for the whole and local contours. Finally, the $C_{d,exp}$ calibrated by actual throat diameter d are employed to verify the $C_{d,th}$ calculated by curvature radius R_c, which the $C_{d,exp}$ was obtained at two pVTt facility in National Institute

of Metrology of China (NIM). When the geometric profile of the nozzle meets the requirements of the evaluation criteria, the theoretical model can be used to accurate predict the discharge coefficient within the uncertainty of less than 0.1%.

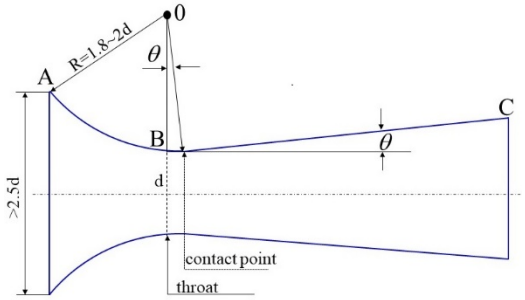

Figure 1: Effect of the parameters on the $C_{d,th1}$.

2. Discharge coefficient of SN

2.1 The theoretical discharge coefficients

As early as 1960s to 1980s, several theoretical or semi-empirical formulas for discharge coefficient have been proposed. In general, the theoretical discharge coefficient (1-C_d) will be divided into three parts: viscous discharge coefficient (1-$C_{d,1}$), inviscid discharge coefficient (1-$C_{d,2}$) and virial discharge coefficient (1-$C_{d,3}$) to obtain accurate flow rate. When the appropriate gas and flow conditions are selected (i.e. dry air without eddy current and near ambient temperature), the value of (1-$C_{d,3}$) is very small and can be neglected.

For (1-$C_{d,2}$), in 1959, Hall firstly calculated the maximum boundary layer displacement thickness as for a semi-infinite plate with zero longitudinal pressure gradient by equating the boundary layer of SN to a uniform circular tube with length L and ignoring the transverse curvature of the boundary layer. Unfortunately, the maximum boundary layer displacement thickness was obtained directly from the boundary layer theory of plate, which leads to a lower accuracy of calculation. Up to 1962, He further analysed the effect of multi-dimensional feature of transonic flow and used a perturbation series expansion in powers of 1/R (R=2R_c/d) to solve the steady, irrotational, axisymmetric, compressible flow equation in the transonic regime, and ulteriorly proposed the formula of the inviscid discharge coefficient, as seen Equation (1) as an example. Remarkably, for sufficiently small R, Hall's solution yields nonphysical results, predicting negative values of the inviscid discharge coefficient. In 1969, Kliegel and Levine found an error in Hall's original solution, and provided a modification, as shown in Equation (2), with a difference of about 0.06% before and after correction. In addition, they extended and improved Hall's work for inviscid discharge coefficient by using a perturbation series solution expanded about 1/(1+R) that converges for all values of R, seen the Equation (3).

$$(1-C_{d,2})=\frac{\gamma+1}{(2R_c/d)^2}\left(\frac{1}{96}-\frac{8\gamma+21}{4608(2R_c/d)}+\frac{754\gamma^2+1971\gamma+2007}{552960(2R_c/d)^2}\right) \quad (1)$$

$$(1-C_{d,2})_{mo}=\frac{\gamma+1}{(2R_c/d)^2}\left(\frac{1}{96}-\frac{8\gamma+21}{2304(2R_c/d)}+\frac{754\gamma^2+2123\gamma+2553}{552960(2R_c/d)^2}\right) \quad (2)$$

$$(1-C_{d,2})_{KL}=\frac{\gamma+1}{(1+2R_c/d)^2}\left(\frac{1}{96}-\frac{8\gamma-27}{2304(1+2R_c/d)}+\frac{754\gamma^2-757\gamma+3633}{276480(1+2R_c/d)^2}\right) \quad (3)$$

For (1-$C_{d,1}$), in 1971, Geropp independently developed an equation of axisymmetric compressible boundary layer under adiabatic conditions by using the similarity transformations, and obtained the accurate analytical solution of the (1-$C_{d,1}$) for the laminar flow boundary layer of SN, as shown in Equation (4). Then, in 1987, under the $\Delta T_w \neq 0$ and Pr≠1, Geropp also put forward (1-$C_{d,1}$) with wall heat transfer, and it is defined by Equation (5).

$$(1-C_{d,1})=\frac{4\left(\frac{\gamma+1}{2}\right)^{\frac{1}{2(\gamma-1)}}}{\sqrt{Re\cdot m}}\left(3\sqrt{2}-2\sqrt{3}+\frac{\gamma-1}{\sqrt{3}}\right),\ \Delta T_w=0,\ Pr=1 \quad (4)$$

$$(1-C_{d,1})_{he}=\frac{4\sqrt{6}b^{1/2}\left(\frac{\gamma+1}{2}\right)^{\frac{1}{2(\gamma-1)}}}{\sqrt{\mathrm{Re}\cdot m}}\left\{\left(1+\frac{\mathrm{m}_T}{\mathrm{m}}\sqrt{\mathrm{Pr}}\right)\cdot\left(\sqrt{3+\frac{3\mathrm{m}_T}{2\mathrm{m}}}-\sqrt{2+\frac{3\mathrm{m}_T}{2\mathrm{m}}}\right)+\frac{(\gamma\text{-}1)\sqrt{\mathrm{Pr}}}{6}\sqrt{2+\frac{3\mathrm{m}_T}{2\mathrm{m}}}\right\},\Delta T_w\neq 0,\ Pr\neq 1 \quad (5)$$

2.2 The experimental discharge coefficients

On of assuming a one-dimensional isentropic flow of an ideal gas, the ideal mass flow q_{mi} through the sonic nozzle, can be expressed as,

$$q_{mi}=\frac{AC_* p_0}{\sqrt{(R_u/M)T_0}} \quad (6)$$

Where, A is the area of throat; m^2, $C_*$is the critical flow function; p_0 is the stagnation pressure, Pa; T_0 is the stagnation temperature, K; R_u is the universal gas constant, J/kmol/K; M is the molecular mass, kg/kmol.

The $C_{d,exp}$ describes this difference between the real mass flow q_{mr} and the ideal mass flow,

$$C_{d,\exp}=\frac{q_{mr}}{q_{mi}} \quad (7)$$

3. Evaluation criterion of contour

Under adiabatic conditions, it shows that the change of $C_{d,th1}$ is less than 0.08% with the throat diameter changes by 3.0% for different throat diameters nozzles. The smaller the throat diameter, the greater the relative variation of $C_{d,th1}$ is. In this experiment, the relative change of $C_{d,th1}$ was less than 0.01% when the change of throat diameter was 0.5% for the nozzle with d=7.45 mm. In addition, it can be seen that the $C_{d,exp}$ is proportional to the square of diameter based on Equation (6) and Equation (7). When the uncertainty of throat diameter is 0.05%, the uncertainty of $C_{d,exp}$ will be 0.1%. Obviously, the accurate value of throat

diameter d is more important for calculating $C_{d,exp}$, which has been verified by experimental data.

Based on Hall-Geropp theory with adiabatic, the effect of R_c on $C_{d,th1}$ can be obtained. It found that the $C_{d,th1}$ decreases with the increase of R_c. When the R_c changes by 1.5d%, the change of $C_{d,th}$ is less than 0.02%. Furthermore, it can also be seen that the larger the throat diameter, the weaker the dependence of $C_{d,th1}$ on R_c is, which can tolerate greater uncertainty. The uncertainty of R_c of 10% or less was acceptable to ensure that the uncertainty of predicted discharge coefficient was less than 0.01% for the nozzle of d=7.45 mm.

Besides, the waviness profile of the nozzle also needs to be evaluated. The waviness profile is expressed as a kind of uneven surface which is larger than mean roughness Ra and smaller than the error of curve profile. It is an intermediate geometry error between micro and macro error. Therefore, the maximum height of waviness profile near the throat w_t, should be $1.5\times10^{-5}d < w_t < 0.1d$.

Based on above analysis and ISO 9300 standard, the deviations of the contour parameters are listed as follows, a) The inlet diameter should differ not more than ±0.001d from the ideal toroidal form; b) The R_c should be within 1.8d to 2.2d; c) The deviation of curve contour between the actual and the ideal at the location of front and back throat of 1 mm should be less than ±0.005d and the deviation of the rest should not exceed ±0.1d. d) The maximum height of waviness profile near the throat wt, should be $1.5\times10^{-5}d < w_t < 0.1d$.

4. Experimental facility and measurement scheme

4.1 The details of experimental apparatus

The nozzles were tested by two pVTt gas flow standard facilities constructed in 1986 and 2014 respectively at NIM, China. One apparatus with the expanded uncertainty of 0.10%~0.20% (k=2) is used to calibrate the discharge coefficient of SN with the flow rates range from 1 m^3/h to 1138 m^3/h at the stagnation pressure of 0.1 MPa. Another apparatus based on the positive pressure method had been constructed as shown in Fig.3. This pVTt facility utilizes a dry compressed air to calibrate the discharge coefficients of sonic nozzles covering flow range extending from 0.019 kg/h to 1367 kg/h, and the stagnation pressure range from 0.1 MPa to 2.5 MPa. The expanded uncertainty of apparatus could be 0.06% (k=2), while the expanded uncertainty of discharge coefficient of calibrated SN was 0.08% (k=2) [8]-[9].

In this study, the nozzles with nominal throat diameter of d=7.45 mm, R_c=2d, diffusion angle of 4° and total length of 48.5 mm are measured and analysed.

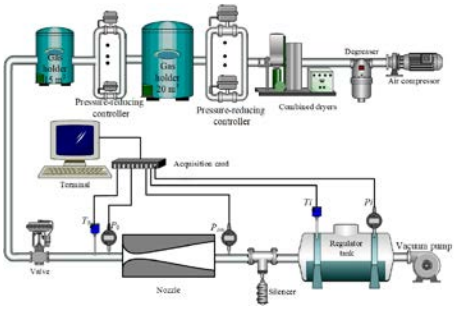

Figure 2: The positive pressure method pVTt facility

The geometry profile of the d=7.45 mm nozzle is measured by using a Leitz $3D^d$ coordinate measurement machine (CMM). The standard uncertainty (k=1) of length measurements made using this CMM is (0.6+l/600) μm where the length dimension of l is in millimetres. The motion range of a CMM is 1200mm×1000mm×700mm. The expanded uncertainty of the throat diameter measurement is estimated to be 1 μm (k=2). This machine is housed in a temperature controlled environment that is maintained at (20±0.01) °C to provide thermal stability. The diameter of the probe selected in this measurement is 3 mm.

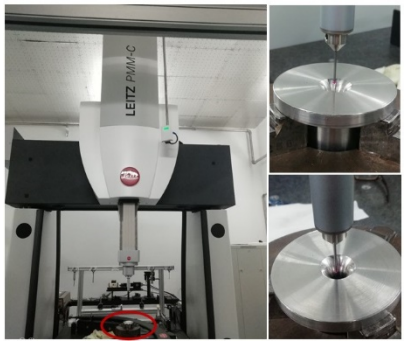

Figure 3: The CMM and ruby probing

4.2 The measurement method

A large number of profile data of nozzles are collected by CMM, instead of throat radius and curvature radius calculated by relative position of finite points, so the profile of SN can be evaluated comprehensively. Both d and R_c are indirectly determined by ruby probe of CMM along the circumference of various cross sections and measuring contours along different azimuthal planes of symmetry. The measurement steps are as follows,

a） Firstly, Cartesian coordinate system is established with nozzle entrance section and axis of nozzle as coordinate Z axis.

b） At each cross section, CMM measurements were taken spaced 30 degrees apart. Each of the eight angles corresponds to a curve along the SN wall that spans from the entrance to the throat, and the measurement step of each arc was 30 μm. These four curves on the axis are used to calculate the R_c.

c） Based on 12 arcs, the approximate position of the smallest circle is found. A total of 25 concentric

circles of each circle about 40 point are generated before and after this position, with an axial interval of 20 μm and a measuring length of 0.5 mm. Least squares regression is used to find the best-fit curve and the average diameter. These diameter at the zero slope location of this fit is taken to be the *d*.

Due to the restriction of measuring rod of CMM, the longest measuring distance of the axis is - 23 mm. In addition, the data measured by CMM is the coordinate value of the probe centre and not the coordinate value of the actual contact point between the probe and the nozzle, so the probe compensation should be carried out, which is corrected according to the normal vector direction of the curve where the point is located.

5. Multi-dimensional contour analysis of SN

5.1 Measurement results of the SN contour

The centre of entrance section and the axis direction of nozzle are taken as coordinate origin and Z axis, respectively. Then along the direction of Z axis for the nozzle of *d*=7.45 mm, 12 arcs are measured at intervals of 30 degree, as shown in Fig.4. These twelve curves well reflect the contour of the SN, and are convenient for calculating its radius of curvature and throat diameter. However, these 12 curves do not compensate for the probe of CMM.

In order to accurately capture the physical dimension of SN, four curves of z1, z4, z7 and z10 are measured repeatedly, and can be corrected according to the probe and eccentricity error of the coordinate machine. The results of the four corrected curves are summarized as shown in Fig.5. As can be seen from Fig.5, these four corrected curves are scattered near the throat of SN due to slightly higher surface roughness caused by the processing method.

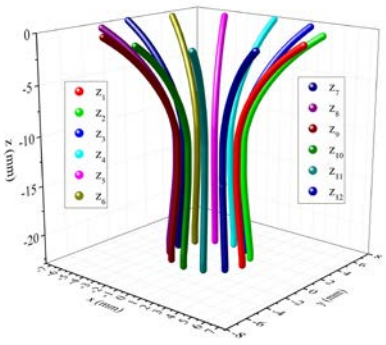

Figure 4: 12 curves of this nozzle.

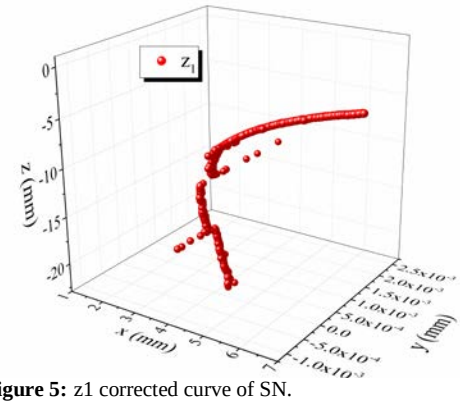

Figure 5: z1 corrected curve of SN.

5.2 Analysis of the SN contour

In order to accurately evaluate whether the contour of SN meets the requirements, it is necessary to analyse the deviation of curves profile and roundness. The three-dimensional curve measured is transformed into two-dimensional curve and compared with the ideal profile, and the comparison result for z1curve is shown in Fig.6 (a). From the Fig.6 (a), the contour around the throat is more like a cylindrical nozzle, and the smallest diameter is located near Z axis of -12.32 mm. Moreover, using the results of these four modified curves, the error of the curve profile is analysed which is expressed as the minimum distance from the each measured points to the ideal curve, and the result is shown in Fig.6 (b).

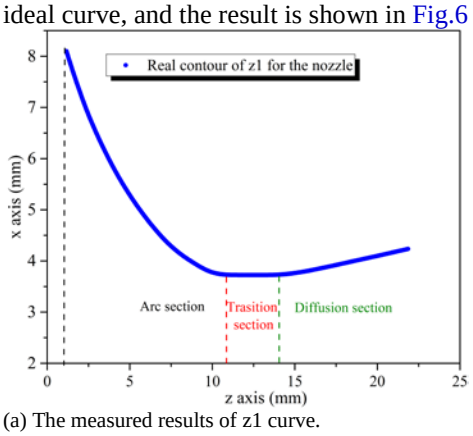

(a) The measured results of z1 curve.

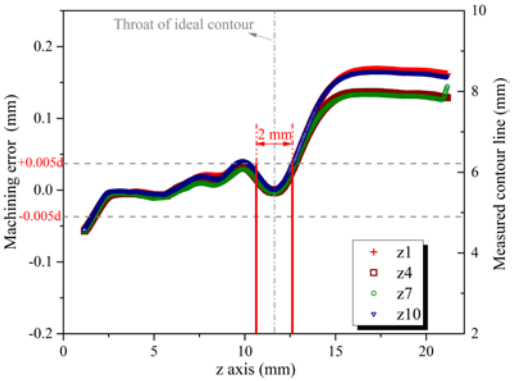

(b) The error of curve contour of z1, z4, z7 and z10.

Figure 6: Sketch of whole curves profile for d=7.45mm nozzle.

It can be seen from the Fig.6 that the line profile error at the entrance and exit is large caused by the angle of attack of the processing probe and the wall angle error. However, it has been proved that the contour in the diffuser 0.1*d* behind the throat has no influence on the discharge coefficient [10]. From the Fig.6, the maximum curve contour error of this nozzle is 0.233 mm<0.1*d* mm. The local line profile error of the front and back 1 mm of the throat is smaller, within the required range of <0.005*d* , which meets the requirements. Therefore, it mainly selected the measuring results at position of less than 1 mm before and after the throat to calculate the *d*, while it selected the results within 8 mm before throat to calculate the R_c.

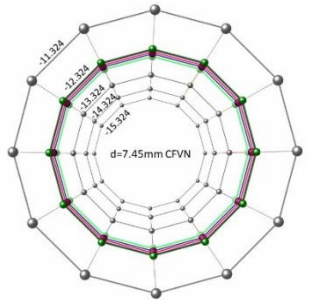

Figure 7: Roundness at five axial positions for d=7.45mm nozzle.

Fig.7 shows cross sectional views of the *d*=7.45 mm SN at different axial distances upstream and downstream of the throat location, according to the 12 points measured 30 degrees apart at each axial location. The figure shows that this nozzle is essentially circular. In addition, the degree of roundness is evaluated by the minimum area method, as shown in Table 1. From Table 1, it can be seen that the maximum degree of roundness is 5.11 μm for this nozzle and is less than ±0.001*d*, which meets the requirements of roundness stipulated in ISO 9300 standard.

Table 1: Roundness of SN at different axial positions.

Number	Axial position (mm)	Degree of roundness (μm)
1	-10.324	5.09
2	-11.324	4.74
3	-12.224	5.06
4	-12.324	4.62
5	-12.424	4.69
6	-12.524	4.92
7	-13.324	5.11
8	-14.324	3.33
9	-15.324	4.09

The contour of sonic nozzle not only needs to meet the requirements of curve profile and roundness, but also needs to meet the waviness requirements. The waviness near the throat of this nozzle is shown in Fig.8, and the sampling length l_w = 1.36 mm. Within the sampling length, the maximum height of the waviness profile is 0.61 μm, which is significantly less than the error of curve profile and roundness and larger than the surface roughness of the normally machined nozzle of 1.5×10^{-5}d.

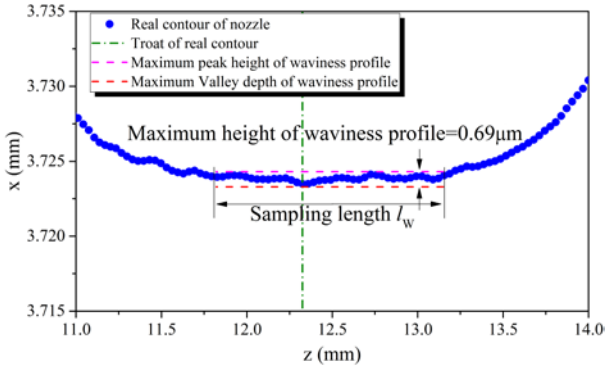

Figure 8: Waviness near the throat for z1 curve.

In conclusion, the whole contour of the nozzle with nominal throat diameter of 7.45 mm meets the geometric requirements. In addition, it found that the throat is located nearly Z axis of -12.32 mm.

5.3 Measurement results of d and R_c

Based on the above analysis, the position of the throat is about - 12.324 mm on Z axis. Therefore, a total of 25 concentric circles were generated before and after this position, with an axial interval of 20 μm and a measuring length of 0.5 mm. Least squares regression is used to find the best-fit curve to calculate the average diameter. The *d*=7.451 mm at Z axis of -12.1537 mm with the zero slope of fitting curve at this location, as shown in Fig.9. The difference between the fitting result and the measured minimum pipe diameter is 0.38 μm, i.e. 0.005%, and its influence on the discharge coefficient is less than 0.01%, which can be neglected.

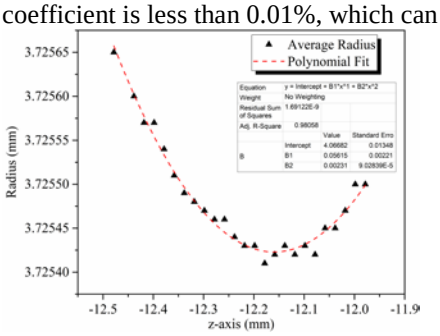

Figure 9: Fit curve of these average radius measurements.

In differential geometry, the reciprocal of curvature is the curvature radius, that is, R_c = 1/K. Taking the minimum diameter (or theoretical minimum diameter) as the throat diameter, 106 points of total of 717 measuring points were selected with 3 mm in front of the throat diameter to calculate the curvature radius.

The mean curvature radius is 14.800 mm by fitting different curves. The difference of curvature radius between fitting and nominal curvature radius is 0.106 mm, i.e. 0.71%, which is far less than the requirement of 10%.

6. Comparison of $C_{d,th}$ with $C_{d,exp}$

Based on the d=7.451 mm, the $C_{d,exp}$ were calibrated on two sets of pVTt gas flow standard facilities, while the $C_{d,th}$ of different models were calculated based on the R_c=14.800 mm. The $C_{d,th}$ is determined by combining Geropp's adiabatic and heat transfer viscous model in laminar boundary layer with modified Hall's inviscid model. The $C_{d,th3}=(1-C_{d,2})_{mo*}(1-C_{d,1})_{he}$ for this SN agreed with $C_{d,exp}$ to better than 0.11% with Pr=0.703, $\Delta T=T_w-T_0$=-5℃ (T_w is wall temperature of nozzle) and γ=1.4, while the overall agreement between $C_{d,th1}=(1-C_{d,2})_{mo*}(1-C_{d,1})$ and $C_{d,exp}$ was better than 0.16% with Pr=1, ΔT=0℃ and γ=1.4, as shown in Fig.10. The measurement Reynolds number Re ranged from 4.45×10^5 to 1.26×10^6, thus the boundary layer at the throat is limited only in laminar. Based on Fig.10, it can be seen that the deviation between $C_{d,th}$ and $C_{d,exp}$ increases with the decrease of Reynolds number. Moreover, it can also be seen that the difference between $(1-C_{d,2})$ and $(1-C_{d,2})_{KL}$ is no more than 0.03%, while the difference between $(1-C_{d,2})_{mo}$ and $(1-C_{d,2})_{KL}$ is less than 0.003%, which is basically the same. In the experimental measurement process, the stagnation temperature T_0 can be stabilized at 20 ℃ for a long time.

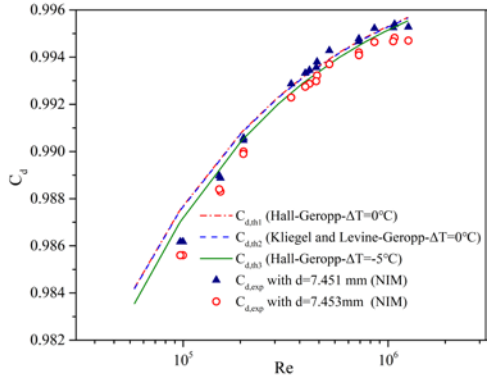

(a) $C_{d,th}$ and $C_{d,exp}$ based on the real and nominal *d*.

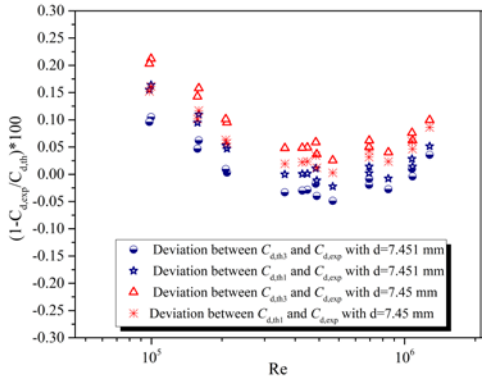

(b) Deviation between $C_{d,th}$ and $C_{d,exp}$.

Figure 10: Comparison between $C_{d,th}$ and $C_{d,exp}$.

7. Conclusion

The *d* and R_c for a sonic nozzle with nominal throat diameter of 7.45 mm were measured by a CMM to calculate the $C_{d,exp}$ and $C_{d,th}$, and corresponding geometric evaluation criteria were established, including curve profile, roundness and waviness. In the range of Re (4.45×10^5~1.26×10^6), the consistency between the $C_{d,exp}$ and the $C_{d,th3}$ was better than 0.11%.

The reliability of the theoretical model of discharge coefficient is verified by comparing the experimental data. Therefore, the theoretical model can be used to predict the discharge coefficient instead of the measured value, when nozzle contour satisfies the requirements of geometry evaluation criteria. In addition, the theoretical discharge coefficient model will not be accurate enough in small Re, and should receive more attentions.

References

[1] B.S. Stratford, The calculation of the discharge coefficient of profiled choked nozzles and the optimum profile for absolute air flow measurement, Journal of the Royal Aeronautical Society, 1964, 68 (640), 237-245.

[2] S.P. Tang et al., Experimental determination of the discharge coefficients for critical flow through an axisymmetric nozzle, AIAA Journal, 1978, 41-46.

[3] D. Geropp, Laminare grenzschichten in ebenen und rotationssymmetrischen lavalduesen, Deutsche luft und raumfahrt forschungsbericht, 1971, 71-90.

[4] I.M. Hall, Transonic flow in two-dimensional and axially-symmetric nozzles, Quarterly Journal of Mechanics and Applied Mathematics, 1962, 15 (4) 487-508.

[5] B.T. Arnberg, et al., Discharge coefficient correlations for circular-arc Venturi flowmeters at critical (sonic) flow, Journal of Fluids Engineering, 1974, 111-123.

[6] M. Ishibashi, M. Takamoto, Discharge coefficient of critical nozzles machined by super-accurate lathes, Proceedings of National Conference of Standards Laboratories, New Mexico, 1998.

[7] W.F. Seidl, Primary calibration of the Boeing 18 kg/s airflow calibration transfer standard, Proceedings of International Symposium on Fluid Flow Measurement, 1986, pp. 80–96.

[8] CH Li, LS Cui, C Wang. The new pVTt facility in NIM. FLOMEKO, Pair, France, 2013.

[9] CH Li, LS Cui, C Wang. The uncertainty analysis and capability verification for the high pressure pVTt gas flow facility of NIM. FLOMEKO, Sydney, Australia, 2016.

[10] M Ishibashi, M Takamoto. Theoretical discharge coefficient of a critical circular-arc nozzle with laminar boundary layer and its verification by measurements using super-accurate nozzles. Flow Measurement & Instrumentation, 2000, 11(4):305-313.